Differential RCS of Multi-Port Tag Antenna with Synchronous Modulated Backscatter

Nicolas Barbot, *Member, IEEE,* Ionela Prodan, *Member, IEEE,* Pavel Nikitin, *Fellow, IEEE,*

***Abstract*—This paper introduces a new method, called multi-port load modulation, allowing one to improve the delta RCS of any passive transponder. By switching simultaneously the loads connected to a multi-port antenna, we show that the associated delta RCS can be higher than the one predicted by the equations of R. Green in 1963. We demonstrate analytically that the delta RCS of the multi-port tag can be improved by 6 dB compared to a single port antenna. This improvement corresponds to an increase of the round-trip read range of 41%. This result can still be improved if the modulation of the structural mode adds constructively with the modulation of the antenna mode. Simulation and measurement of a fully compliant dual-port tag validate the model and achieve a large part of the predicted improvement.**

***Index Terms*—Differential Radar Cross-Section (RCS), EPC Gen2, multi-port antenna, multi-port load modulation, Radio Frequency Identification (RFID).**

I. Introduction

Backscatter communicatons allows a transponder to transfer information at a fraction of the complexity and cost of classical transponders that use active components. Moreover, if the power can be harvested from the electromagnetic wave sent by the reader, fully passive transponders can be designed. RFID technology is the most famous example which is used world wild since more than 20 years now.

In the past, read ranges of RFID systems were limited by the tag sensitivities, thus most of the research effort was oriented to reduce the tag sensitivity. Over the last 20 years, tag sensitivity has been improved by 1 dB per year on average. Today, sensitive chips can be activated with a power as low as -23 dBm. As a result, RFID system performance is no longer solely limited by the tag sensitivity but also by the reader sensitivity [1].

Optimization of the performance when the read range is limited by the reader sensitivity is a recent research topic that will take more importance in the future. The main idea is to maximize the modulated power backscattered by the tag. This power is linked to the backscattered field of loaded antennas which has been understood since 1963 by R. Green [2]. In his thesis, Green successfully decomposed the scattered field of a loaded antenna into two different contributions, which are the structural mode and the antenna mode. The first contribution is the part of the scattered field which is independent of the load connected to the antenna port. The latter contribution is proportional to the reflection coefficient between the antenna and the load and has the same properties as the transmitting antenna. However, unlike other decompositions based on short circuit response [3], [4, Eq. (20)], and on open circuit response [5, Eq. (10)], Green's decomposition is based on complex conjugate response [2, Eq. (14)] and can easily be used to predict and bound all possible scattered field values as a function of the load. These concepts have been used and applied in the RFID technology to estimate the scattered field and the efficiency of the transponders. More specifically, the differential RCS of RFID tags (also known as delta RCS) which has been introduced in [6] and extended in [7], has been derived directly from Green's work.

N. Barbot is with Univ. Grenoble Alpes, Grenoble INP, LCIS, F-26000 Valence, France. P. Nikitin is with Impinj Inc, Seattle, WA, USA.

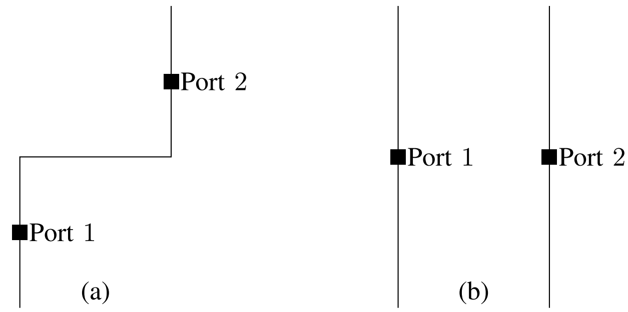

Fig. 1. Example of multi-port antenna composed of two ports: (a) single structure, (b) two separated structures.

The delta RCS associated with a UHF RFID tag which can switch between two states with complex reflection coefficients Γ_1 and Γ_2 is equal to [2, Eq. (32)], [6, Eq. (6)], [7, Eq. (22)]:

$$\sigma_d = \frac{\lambda^2 G^2}{4\pi}\frac{|\Gamma_1 - \Gamma_2|^2}{4} \tag{1}$$

where λ is the wavelength, G is the gain of the antenna and Γ_j is the complex power wave reflection coefficient between the antenna and the load in the considered state:

$$\Gamma_j = \frac{Z_{cj} - Z_a^*}{Z_{cj} + Z_a} \tag{2}$$

As remarked in [6], note that (1) is valid for any antenna and any load. This quantity is also a bound on the modulated power which can be backscattered towards the reader. From (1), we can see that the distance between Γ_1 and Γ_2 can not be higher than 2 since $|\Gamma_i|$ is always lower than 1 for any passive loads. Moreover, for passive tags, this bound is even lowered since the default state has to be matched *i.e.*, $\Gamma_0 = 0$, thus maximum distance can not be higher than 1.

Based on (1) and with the previous assumptions, a classical half-wavelength dipole at 915 MHz has a maximal delta RCS for passive (modulating between match and short) and semi-passive (modulating between open and short) UHF tags of -22.4 dBsm (57.5 cm^2) and -16.4 dBsm (230 cm^2)

This article has been accepted for publication in IEEE Journal of Radio Frequency Identification. This is the author's version which has not been fully edited and content may change prior to final publication. Citation information: DOI 10.1109/JRFID.2025.3557078

respectively. This delta RCS value directly limits the round-trip read range of any UHF tags.

The objective of this paper is to design a new kind of tags with improved delta RCS and round-trip read range. This design relies on the concept of multi-port tag and multi-port antenna. Multi-port tags are not new in the RFID literature [8]–[10]. Usually, these architectures are used to provide diversity in the forward link, which means that if one port experiences a strong attenuation, the other port can still be used to maintain a given performance. However, in the reverse link, all of these works consider that a single port is backscattering at a given time. This condition avoids any collision between different tags and remains a foundation of the RFID protocol.

The proposed multi-port load modulation technique presented in this paper contrasts previous work in that the different ports of the system have to switch at the same time. This can also be seen as a "controlled collision" between different ports which can improve both delta RCS and round-trip read range. This technique is particularly useful for semi-passive tags which are limited by the reader sensitivity. Additionally, this concept has been observed and/or measured experimentally on independent tags in [11]–[14]. Compared to these works, this paper provides the analytic model allowing one to predict the delta RCS as a function of the parameters of the multi-port tag.

This article is an extension of [15]. Compared to the conference paper, this extension includes a generalization of the concepts to N ports (instead of 2) and the addition of a theoretical model based on antenna array theory. Compared to the general model, this simple model neglects the coupling but allows one to easily predict the delta RCS of multi-port antennas composed of several (identical) elements. Moreover, this extension presents for the first time, a tag based on a multi-port antenna with improved delta RCS which is fully compatible with the EPC Gen2 protocol.

II. General Model for a Multi-Port Antenna

In the following, we consider a multi-port antenna which includes N distinct ports. In emission, this antenna can produce an electric field when a voltage (and/or a current) is applied on any of its ports. In reception, this same antenna can generate a voltage (and/or a current) on any of its ports when a wave is impinging the structure. Each port can be loaded by a (passive) complex impedance value. Without any loss of generality, a multi-port antenna can be composed of a single structure or multiple structures, and ports can be placed anywhere on the structure(s) as presented in Fig. 1. The model presented in this section is general and can be applied to any multi-port antenna. Note that the demonstration for a dual-port antenna case is presented in [15].

A. RCS of a Loaded Multi-Port Antenna

The backscattering of fields by a loaded antenna has been known since [2] where Green succeeded to decompose the backscattered field into a structural mode and an antenna mode. This decomposition became famous since that all possible amplitude and phase of the backscattered signal can be

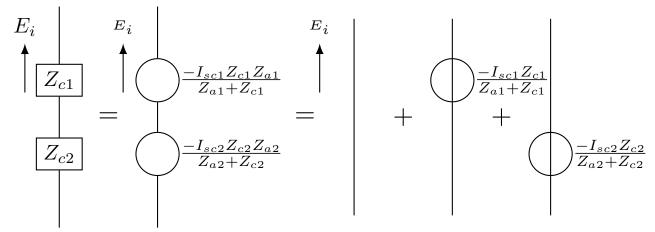

Fig. 2. Decomposition of the field backscattered by a multi-port antenna composed of two ports.

easily predicted from the load connected to the antenna due to Γ being a bounded quantity. Note that this derivation also assumes a single port antenna. Consequently, the delta RCS of a single-port antenna can, by definition, not be higher than (1).

On the other hand, if we consider the delta RCS of an antenna with more than one port, then this quantity is, by design, not bounded by (1) if loads on all ports can be switched at the same time. The rest of this section generalizes the procedure discovered by Green in the case of a multi-port antenna.

By using the compensation theorem and then the superposition theorem, the field backscattered by a multi-port antenna can be decomposed into the field backscattered by the antenna with a short circuit on all ports plus the field generated by each port loaded by a voltage generator while the other ports are short circuited (see Fig. 2):

$$E_s(Z_{c1},\cdots,Z_{cN}) = E_s(0,0,\cdots) - \sum_{i=1}^{N} \frac{Z_{ci} I_{sci}}{Z_{ci}+Z_{ai}} E_{ri} \quad (3)$$

By using (3) with a conjugate matching on all ports, we can express $E_s(0,0,\cdots)$ as:

$$E_s(0,0,\cdots) = E_s(Z_{a1}^*,\cdots,Z_{aN}^*) + \sum_{i=1}^{N} \frac{Z_{ai}^*}{2R_{ai}} I_{sci} E_{ri} \quad (4)$$

Also, short-circuit current on port i, I_{sci} can be expressed as a function of the conjugate currents:

$$I_{sci} = I_i(Z_{ai}^*) \frac{2R_{ai}}{Z_{ai}} \quad (5)$$

Thus, $E(0,0,\cdots)$ can be expressed only with the conjugate currents:

$$E_s(0,0,\cdots) = E_s(Z_{a1}^*,\cdots Z_{aN}^*) + \sum_{i=1}^{N} \frac{Z_{ai}^*}{Z_{ai}} I_i(Z_{ai}^*) E_{ri} \quad (6)$$

Finally, (6) can be substituted into (4) to obtain:

$$\begin{aligned} E_s(Z_{c1},\cdots,Z_{cN}) &= E_s(Z_{a1}^*,\cdots,Z_{aN}^*) \\ &+ \sum_{i=1}^{N} \frac{1}{Z_{ai}} \left[Z_{ai}^* + \frac{2R_{ai}Z_{ci}}{Z_{ai}+Z_{ci}} I_i(Z_{ai}^*) E_{ri} \right] \end{aligned} \quad (7)$$

which can more simply be expressed as:

$$\begin{aligned} E_s(Z_{c1},\cdots,Z_{cN}) &= E_s(Z_{a1}^*,\cdots,Z_{aN}^*) \\ &- \sum_{i=1}^{N} \Gamma_i I_i(Z_{ai}^*) E_{ri} \end{aligned} \quad (8)$$

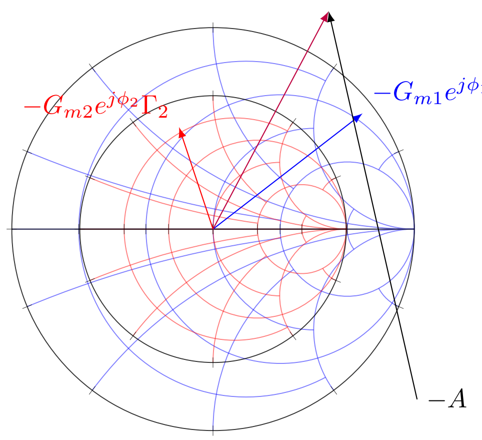

Fig. 3. Graphical representation of the scattering of a multi-port antenna composed of two ports. The figure is composed of two Smith charts corresponding to the two antenna modes. Square root of the RCS of the dual-port antenna is proportional to the length of the black plain line.

where Γ_i is the reflection coefficient at the considered port i:

$$\Gamma_i = \frac{Z_{ci} - Z_{ai}^*}{Z_{ci} + Z_{ai}} \tag{9}$$

The RCS of the multi-port antenna can finally be extracted:

$$\sigma = 4\pi r^2 \frac{|E_s(Z_{a1}^*, Z_{a2}^*) - \sum_{i=1}^{N} \Gamma_i I(Z_{ai}^*) E_{ri}|^2}{|E_i|^2} \tag{10}$$

This RCS can also be expressed as a function of antenna "gains" G_{mi}.

$$\sigma = \frac{\lambda^2}{4\pi} \cdot \left| A - \sum_{i=1}^{N} G_{mi} e^{j\phi_i} \Gamma_i \right|^2 \tag{11}$$

with:

$$A = \frac{4\pi}{\lambda} E_s(Z_{a1}^*, \cdots, Z_{aN}^*) \tag{12}$$

$$G_{mi} = \frac{4\pi}{\lambda} |I_i(Z_{ai}^*) E_{ri}| \tag{13}$$

$$\phi_i = \arg(I_i(Z_{ai}^*) E_{ri}) \tag{14}$$

Note that G_{mi} are not equal to the gains of the antenna at port i but are different quantities. Fig. 3 presents the different quantities graphically. Note that the structural mode is not bounded and can be inside or outside any Smith charts. The antenna mode of port i is bounded by a circle of radius G_{mi}. These two circles are represented by the two Smith charts and each antenna mode can not be outside its respective circle. The total antenna mode corresponding to the summation of each port is bounded by a radius of $\sum_{i=1}^{N} G_{mi}$. Finally the square root of the RCS of the multi-port antenna is proportional to the length between $-A$ and the total antenna mode.

B. Delta RCS of a multi-Port Tag

Let's now imagine that each port of this multi-port antenna can be switched between two values:

$$\begin{cases} Z_{c1} \to (Z_{c11}, Z_{c12}) \\ Z_{c2} \to (Z_{c21}, Z_{c22}) \\ \quad \vdots \\ Z_{cN} \to (Z_{cN1}, Z_{cN2}) \end{cases} \tag{15}$$

Note that the impedance change have to takes place at the same time on all ports. This condition is particularly important because if a single port is switched at a given time, the delta RCS associated to each variation is directly given by (1) and can not be improved.

By applying (8) for both states and then doing the difference, the total field variation can be obtained by:

$$\begin{aligned} \Delta E_s = {} & E_s(Z_{a11}^*, \cdots, Z_{aN1}^*) - E_s(Z_{a12}^*, \cdots, Z_{aN2}^*) \\ & - \sum_{i=1}^{N} \Gamma_{i1} I_i(Z_{ai1}^*) E_{ri1} + \sum_{i=1}^{N} \Gamma_{i2} I_1(Z_{ai2}^*) E_{ri2} \end{aligned} \tag{16}$$

The quantity expressed by (16) can be normalized to obtain the delta RCS of the multi-port antenna:

$$\begin{aligned} \sigma_d = {} & \pi r |E_s(Z_{a11}^*, \cdots, Z_{aN1}^*) - E_s(Z_{a12}^*, \cdots, Z_{aN2}^*) \\ & + \sum_{i=1}^{N} \Gamma_{i2} I_i(Z_{ai2}^*) E_{ri2} - \sum_{i=1}^{N} \Gamma_{i1} I_i(Z_{ai1}^*) E_{ri1}|^2 / |E_i|^2 \end{aligned} \tag{17}$$

Equation (17) can also be expressed as a function of the "gains" G_m:

$$\begin{aligned} \sigma_d = \frac{\lambda^2}{16\pi} \Bigg| & A_1 - A_2 \\ & + \sum_{i=1}^{N} G_{mi2} e^{j\phi_{i2}} \Gamma_{i2} - \sum_{i=1}^{N} G_{mi1} e^{j\phi_{i1}} \Gamma_{i1} \Bigg|^2 \end{aligned} \tag{18}$$

with:

$$A_j = \frac{4\pi}{\lambda} E_s(Z_{a1j}^*, \cdots, Z_{aNj}^*) \tag{19}$$

$$G_{mij} = \frac{4\pi}{\lambda} |I_{ij}(Z_{aij}^*) E_{rij}| \tag{20}$$

$$\phi_{ij} = \arg(I_{ij}(Z_{aij}^*) E_{rij}) \tag{21}$$

Equation (18) is the general form of the delta RCS of a multi-port antenna. The term $A_1 - A_2$ is a modulation due to the variation of the structural mode between the two states. This term was not present for single-port antenna [see (1)]. Each following term is proportional to Γ_{ij} and corresponds to the modulation of the antenna mode produced by each port. The direct analysis of (18) states that if we can find a dual-port antenna having good "gains" on both ports ($G_{mij} \approx G$), then delta RCS of a dual-port antenna can potentially be improved by a factor of 4 (*i.e.* +6 dB) each time the number of ports is multiplied by 2 provided that last two terms in (18) have the opposite phase. This result can still be improved if the modulation due to the structural mode adds constructively. In terms of read range, assuming a free space environment, each

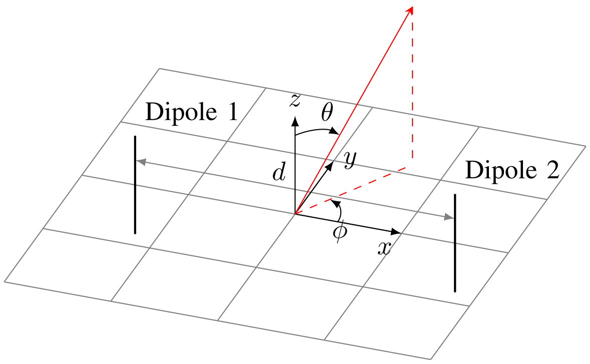

Fig. 4. Geometry of the two dipoles impinged by a plane wave.

increase of the delta RCS of 6 dB represents an improvement of 41% of the round trip read range [1] which is very significant for overall RFID system performance.

III. Model without Coupling for a Multi-Port Antenna

The previous section provides a model which is valid for any multi-port antenna. Ports can be on the same or different structures as presented in Fig. 1(a) and (b). However, this model remains complex to use in practice since when one load is changed at a given port, it can affect the parameters of any other ports. To provide a simpler model, we reduce the multi-port antenna to N identical structures spatially separated in space [like in Fig. 1(b)]. Moreover, we assume that these structures are not coupled, *i.e.*, the current induced on a structure does not affect the current of another structure. With these assumptions, the backscattered field of the multi-port antenna can be obtained by adding the backscattered field produced by each element taken separately. Note that these antennas represent only a small subset of the multi-port antennas described in Section II. The rest of this Section presents the simple case of a dual-port antenna. The generalization to multi-port antennas is presented at the end of the Section.

A. RCS of a Loaded Multi-Port Antenna

To illustrate the approach, let us consider that the multi-port antenna is composed of two dipole antennas separated by a distance d. Fig. 4 presents the configuration and the notation used in the following. In the farfield zone of the multi-port antenna, the total backscattered field can be approximated by:

$$E_s(Z_{c1}, Z_{c2}) \approx E_{s0}(Z_{c1})e^{+jkd\cos\theta} + E_{s0}(Z_{c2})e^{-jkd\cos\theta} \quad (22)$$

where $E_{s0}(Z_c)$ is the scattered field of a single dipole located at the origin. From Green's thesis, we know that the field scattered by a single-port antenna is equal to [2]:

$$E_{s0}(Z_c) = E_{s0}(Z_a^*) - \Gamma I_0(Z_a^*)E_{r0} \quad (23)$$

Substituting (23) into (22) leads to:

$$E_s(Z_{c1}, Z_{c2}) = E_{s0}(Z_a^*)2\cos[kd\cos\theta] - I_0(Z_a^*)E_{r0}\left[\Gamma_1 e^{+jkd\cos\theta} + \Gamma_2 e^{-jkd\cos\theta}\right] \quad (24)$$

Note that this formula is a simplified form of [15, Eq. (11)] [see also (8)]. Moreover when $\Gamma_1 = \Gamma_2$, (24) takes the following simple form:

$$E_s(Z_{c1}, Z_{c2}) = [E_{s0}(Z_a^*) - \Gamma_1 I_0(Z_a^*)E_{r0}] \times 2\cos[kd\cos\theta] \quad (25)$$

where we can recognize the field scattered by a single dipole at the origin multiplied by a factor which depends on the geometry of the multi-port antenna. Equations (24) and (25) are actually similar to the antenna array theory [16, p. 249]. A special attention has to be paid that, in the general case *i.e.*, when $\Gamma_1 \neq \Gamma_2$, the array factor for the structural mode and for the antenna mode are different. These two quantities are equal only when $\Gamma_1 = \Gamma_2$.

From (24), the RCS of the dual-port antenna can be estimated by:

$$\sigma = \frac{\lambda^2 G^2}{4\pi} \cdot |A - e^{j\phi_1}\Gamma_1 - e^{j\phi_2}\Gamma_2|^2 \quad (26)$$

with:

$$A = \frac{E_{s0}(Z_a^*)}{I_0(Z_a^*)E_{r0}} 2\cos[kd\cos\theta] \quad (27)$$

$$\phi_i = \pm kd\cos\theta \quad (28)$$

and G the gain of the single element located at the origin. Note that this formula is a simplified form [15, Eq. (14)] [see also (11)].

B. Delta RCS of a Loaded Multi-Port Antenna

If we now assume that each port can switch (simultaneously) between two impedance values, the total field variation can be obtained by:

$$\Delta E_s = -I_0(Z_a^*)E_{r0} \times \left[(\Gamma_{11} - \Gamma_{12})e^{-jkd\cos\theta} + (\Gamma_{21} - \Gamma_{22})e^{+jkd\cos\theta}\right] \quad (29)$$

Note that this formula is a simplified form [15, Eq. (19)] [see also (16)]. Finally, the associated delta RCS can finally be obtained by:

$$\sigma_d = \frac{\lambda^2 G^2}{16\pi} \cdot \left|(\Gamma_{11} - \Gamma_{12})e^{-jkd\cos\theta} + (\Gamma_{21} - \Gamma_{22})e^{+jkd\cos\theta}\right|^2 \quad (30)$$

Note that this formula is a simplified form of [15, Eq. (21)] [see also (18)] which can easily be used to predict the delta RCS of an array of loaded antennas. Moreover, compared to (18), the structural mode modulation can not be predicted by this simple model since the coupling is not taken into account. Finally, in the case where this multi-port tag is loaded by loads satisfying $\Gamma_{11} - \Gamma_{12} = \Gamma_{21} - \Gamma_{22}$, *e.g.*, using identical chips at both ports, σ_d can be written as:

$$\sigma_d = \frac{\lambda^2 G^2}{16\pi} \cdot |\Gamma_{11} - \Gamma_{12}|^2 4\cos^2[kd\cos\theta] \quad (31)$$

where we can easily see that the delta RCS can be improved by 6 dB compared to the single-port antenna composed with a single element. Remember that this equation does not

This article has been accepted for publication in IEEE Journal of Radio Frequency Identification. This is the author's version which has not been fully edited and content may change prior to final publication. Citation information: DOI 10.1109/JRFID.2025.3557078

consider the structural mode modulation due to the coupling between the two elements. Finally, the approach can easily be generalized to N ports antenna composed of N (identical) elements by recognizing the delta RCS of a single element multiplied by the magnitude squared of the array factor:

$$\sigma_d = \sigma_{d0} \cdot |AF|^2 \tag{32}$$

where σ_{d0} is the delta RCS of a single element and AF is the array factor of the structure. Note that (32) is only valid when $\Gamma_{11} - \Gamma_{12} = \Gamma_{21} - \Gamma_{22}$ *e.g.*, using identical chips at both port. If this condition on the reflection coefficient can not be satisfied, a generalization of (30) for the considered array has to be used instead.

IV. Simulation

In this section, we still consider the two dipoles impinged by a plane wave (see Fig. 4). Simulations have been realized with NEC2, which is based on the Method of Moments numerical simulation method. Each dipole has a length of 15 cm which is approximately equal to $\lambda/2$ at 915 MHz and has been modeled by 11 segments using the thin wire approximation. Moreover, each dipole can be loaded at its center by a complex load. Default state has been chosen at $Z_{c11} = Z_{c21} = 10 + 100i\ \Omega$. A plane wave impinges the structure with an angle (θ, ϕ) and scattered field is collected using a farfield probe in the same direction at a distance of 1 m.

The first study compares the two models proposed previously and the simulation using NEC2. The first model takes into account the coupling whereas the second one is simpler and assumes no coupling. Determination is based on (8) and (25) for first and second model respectively. Moreover, for the first model, independent simulations have been performed to determine the values of each parameter (*i.e.*, Z_{ai}, Γ_i, E_{ri}, $I_1(Z^*_{aij})$. The scattered field is extracted for $(\theta = \pi/2, \phi = 0)$ as a function of the distance d between the dipoles. Results are presented in Fig. 5 where we can see that the simulation and the general model of the scattered field [see (8)] are in a very good agreement (slight difference appears at the second digit after the comma). Note that for this two dipoles arrangement, the coupling can be expressed analytically [16, p. 412]. However, analytical model for coupled elements is not known for general structure (*i.e.*, other than dipoles). The simple model without coupling produces a less accurate results especially when the distance between the two dipoles is small due to the strong coupling between the two dipoles. For longer distances (typically more than few wavelengths), the simple model can easily replace the general model to predict the scattered field.

In the second study, both ports are switched simultaneously (from $Z_{c11} = Z_{c21} = 10 + 100i\ \Omega$ to $Z_{c12} = Z_{c22} = 10 - 100i\ \Omega$). Delta RCS is extracted by using two independent simulations (one in each state) and compared to both models (with and without coupling), with the results presented in Fig. 6. Here again, we can see that the general model perfectly fits the simulation. Simple model provides a good approximation only when the distance between the two dipoles is higher that few wavelength. Below this distance, simple model cannot be used accurately.

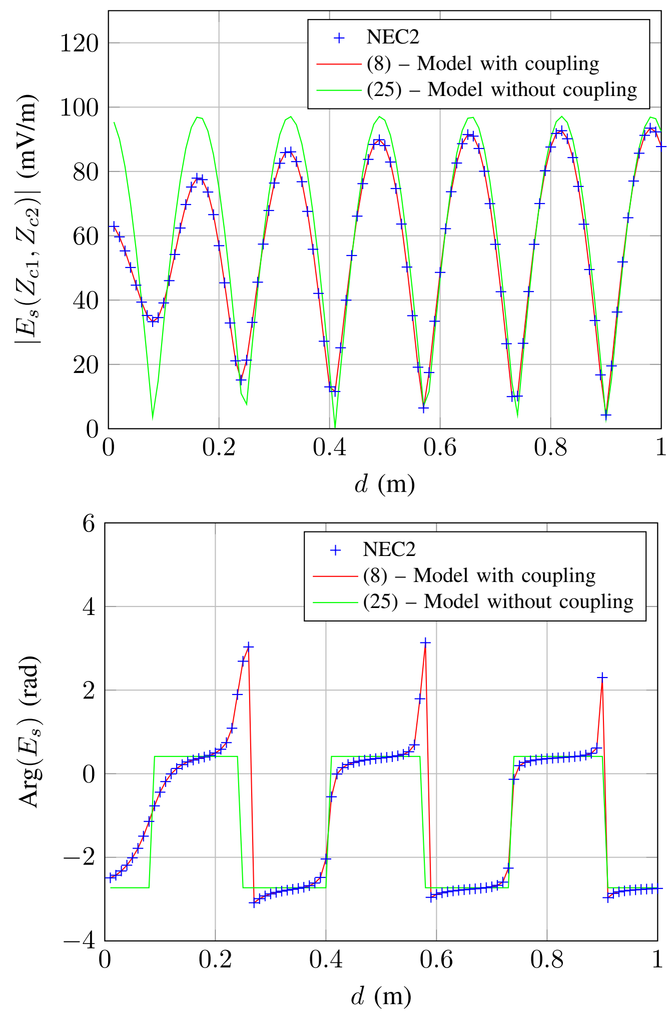

Fig. 5. (a) Magnitude and (b) phase of the scattered field (in the first state) as a function of the distance between the two dipoles.

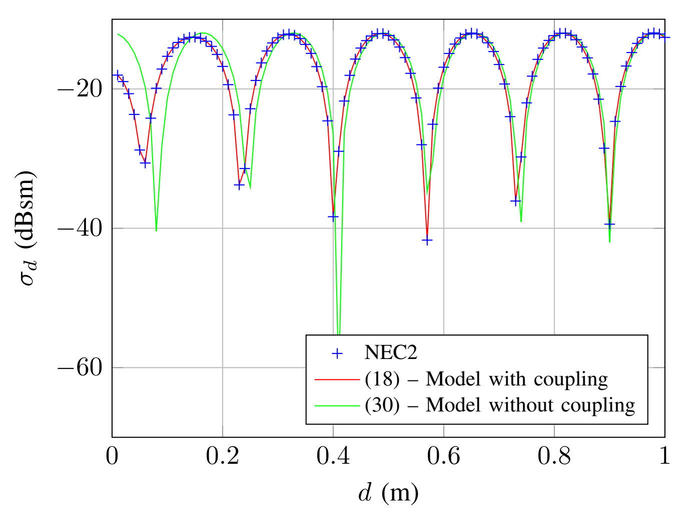

Fig. 6. Delta RCS as a function of the distance between the two dipoles when the two ports are switched simultaneously.

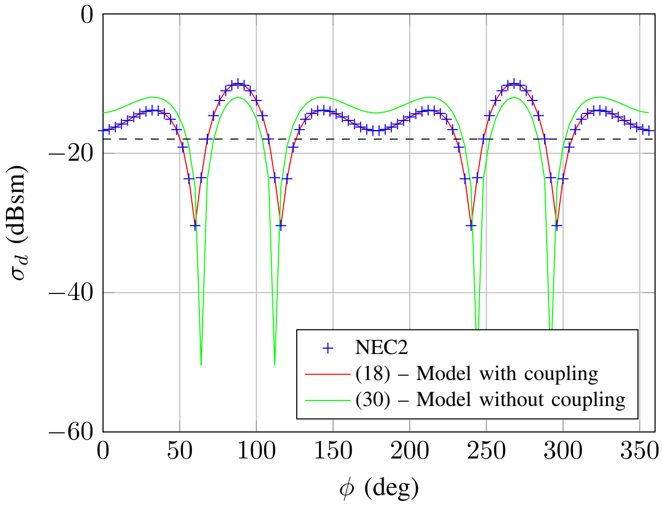

Fig. 7. Delta RCS as a function of the angle ϕ when the two ports are switched simultaneously.

Finally, delta RCS is plotted, for a fixed distance of $d = 20$ cm between the two dipoles, for $\theta = \pi/2$ and for all ϕ values. Results are presented in Fig. 7. Here again, the general model is in perfect agreement with the simulation. The simple model without coupling is able to predict the delta RCS with an accuracy of 2 dB (for this specific d value). Higher accuracy can be obtained for lager distances. Moreover, Fig. 7 also presents, in dashed line, the delta RCS of a single port antenna composed of a single dipole and switching with the same impedance values (from $Z_{c1} = 10 + 100i\ \Omega$ to $Z_{c2} = 10 - 100i\ \Omega$). In this specific case the delta RCS is independent of ϕ and equal to -17.96 dBsm. Thus we can see that the delta RCS of a multi-port antenna can be improved compared to a single-port antenna composed with the same element. From Fig. 7, for $\phi = \pi/2$ the maximum delta RCS predicted by the simple model is -11.96 dBsm, which is exactly 6 dB higher than the single port antenna. More interestingly, the maximum predicted by the general model (and by the simulation) is equal to -9.98 dBsm (see also Table 2 in [15]). This represents an improvement of 8 dB compared to the single-port antenna where 6 dB are due to the increased gain and 2 dB are due to the structural mode modulation (*i.e.*, the coupling between the two elements). This result is significant for future design of new RFID tags with improved delta RCS.

V. Optimization of the Impedance Values

For a given N-port antenna, an interesting question arises of how to optimize the $2N$ impedance values to maximize the delta RCS. This optimization can be done based on the two previously presented models leading to two different approaches. In the following, we consider the previously studied multi-port antenna composed of two dipoles separated by a distance of 20 cm. The reader is assumed to be placed facing to the dipoles (*i.e.*, $\theta = \pi/2$, $\phi = \pi/2$). Different multi-port antennas and configuration can be addressed using the same approach.

TABLE I
Optimization of the states of dual-port tag at 915 MHz.

	Time slot 1	Time slot 2
Z^0_{c1j} (Ω)	$20 + 0i$	$30 - 100i$
Z^0_{c2j} (Ω)	$50 + 100i$	$100 + 0i$
Z_{a1} (Ω)	$61.69 - 25.79i$	$64.04 - 27.62i$
Z_{a2} (Ω)	$63.16 - 30.80i$	$66.82 - 28.31i$
ϕ_{1j} (rad)	-1.910	-1.830
ϕ_{2j} (rad)	-1.7713	-1.7570
$\arg(A_1 - A_2)$ (rad)	-1.942	
Γ_{1j}	$-0.9923 - 0.1239i$	$0.9932 - 0.1165i$
Γ_{2j}	$-0.9875 + 0.1576i$	$0.9831 - 0.1833i$
Z_{c1j} (Ω)	$0 + 26.76i$	$0 - 1114i$
Z_{c2j} (Ω)	$0 + 36.19i$	$0 - 692.9i$
σ_d (dBsm)	-7.153	

A. Model without coupling

For the model based on an antenna array (see Section III), the procedure is trivial. Assuming $\Gamma_{11} = \Gamma_{21}$ and $\Gamma_{11} = \Gamma_{21}$, maximization of (30) can be achieved by choosing any Γ_{i1} and Γ_{i2} values such that:

$$|\Gamma_{i1} - \Gamma_{i2}| = 2 \tag{33}$$

which means that the two points have to be placed on a diameter of the modified Smith chart. Note that if the multi-port tag has to harvest the power from the reader, the default states on each ports have to be matched *i.e.*, at the center of the modified Smith chart. Note that the procedure is equivalent to the optimization of the loads of a single-port tag. The achieved delta RCS of the multi-port antenna is, in this case, 6 dB higher than the delta RCS of a single element. Thus, based on the simple model, the maximum achievable delta RCS for the multi-port antenna considered in Section IV is equal to $-16.4 + 6 = -10.4$ dBsm.

B. General model

This model is more complex but also more accurate than the simple model based on an antenna array since it takes into account the coupling between the elements.

In this case, the objective of the optimization procedure is to align each antenna mode terms to the structural mode in order to obtain a (constructive) summation. Assuming that the antenna parameters (*i.e.*, A_1, A_2 and ϕ_{ij}) are known, Γ_{ij} values have to chosen such such that:

$$\arg(A_1 - A_2) = \phi_{ij} + \arg(\Gamma_{ij}) \tag{34}$$

Moreover, choosing $|\Gamma_{ij}| = 1$ to maximize the distance variation leads to:

$$\Gamma_{ij} = e^{j(A_1 - A_2 - \phi_{ij})} \tag{35}$$

Finally, knowing Γ_{ij}, the associated impedance values can be extracted with:

$$Z_{cij} = \frac{Z_{aij}\Gamma_{ij} + Z^*_{aij}}{-\Gamma_{ij} + 1} \tag{36}$$

It is interesting to notice that the determination of A_1, A_2, ϕ_{ij} and Z_{aij} requires the knowledge of the impedance values.

This article has been accepted for publication in IEEE Journal of Radio Frequency Identification. This is the author's version which has not been fully edited and content may change prior to final publication. Citation information: DOI 10.1109/JRFID.2025.3557078

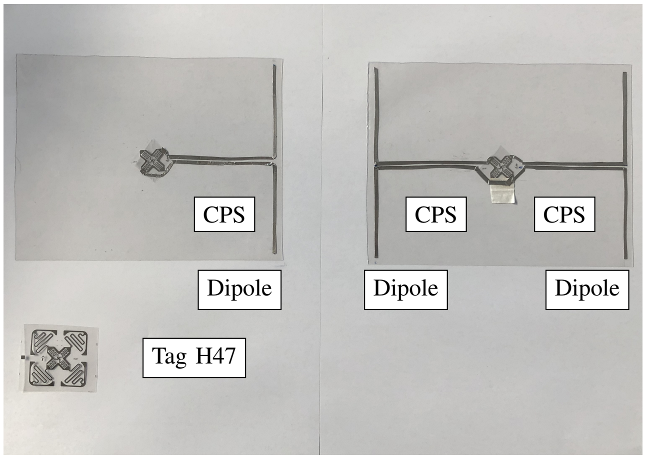

Fig. 8. Photograph of the tags used in the study. Left: single-port tag. Right: multi-port tag. The original H47 tag based on the Monza 4D chip is presented for reference.

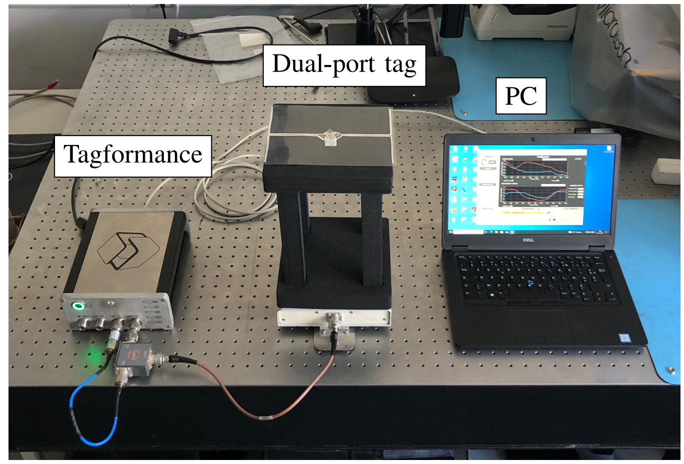

Fig. 9. Photograph of the proposed bench based on the Voyantic Tagformance reader in real environment.

Thus, in order to apply (35), an initial impedance set values, called Z^0_{cij}, is first chosen to estimate the antenna parameters. Then Γ_{ij} and Z_{cij} are computed based on the antenna parameters. Note that, if the coupling is important, (35) can be applied iteratively (by carefully re-computing the antenna parameters). Results of this procedure are presented in Table I and shows that maximum delta RCS can reach -7.1 dBsm. This result has been obtained using a single iteration of the algorithm. Direct comparison with the antenna array theory indicates that the coupling plays an important role and allows the tag designer to obtain an improvement of $10.4 - 7.1 = 3.3$ dB compared to the antenna array theory.

VI. Fully Compliant UHF Multi-Port Tag

A. Dual-Port Tag

Dual-port tags can be realized using at least two backscatter modulators. Designs can be obtained from [17] for example by adding a second backscatter modulator. Moreover, in [15], a proof of concept was proposed based on two independent tags. While this approach was able to validate the improvement of the delta RCS, the EPCID value of the multi-port tag has not been read due to the random nature of the RFID protocol. This paper proposes, for the first time, a fully compliant multi-port RFID tag based on

- a commercial UHF chip available off the shelf.
- a homemade aluminum dual-port antenna

Most of the RFID chips only have two pads which are connected to the arms of a dipole-like antenna (usually through a matching structure such as T-matching). However some chips have four pads. For example the Impinj Monza 4 chip has four pads called RF1+, RF1-, RF2+ and RF2-. These four pads work by pairs which means that (RF1+, RF1-) and (RF2+,RF2-) are fully isolated from each other. This design was introduced to achieve an orientation insensitivity of the tag under linear polarization of the reader. By connecting two dipoles oriented at 90° to the two pairs of port, a tag can be activated irrespectively of its orientation. An example of UHF tag designed using this approach, Impinj reference design H47, is presented in the left corner of Fig. 8. Today, these designs are not common since most of the reader antennas use a circular or dual-linear polarization [18].

In this section, a multi-port tag based on a Monza 4 chip fully compliant with the RFID protocol is proposed. Note that, due to the design of the Monza 4 chip, $\Gamma_{1j} = \Gamma_{2j}$ (*i.e.*, it is not possible to have a different load value on each port). The multi-port tag is based on the Impinj reference design H47 (see left corner of Fig. 8) where the two dipoles have been cut away to keep only the T-matching network and the chip. The proposed multi-port tag is based on two dipoles of length 15 cm separated by 20 cm and is, in principle, identical to the design simulated in Section IV. Two transmission lines based on coplanar stripline are used to connect the dipoles to the matching network. A picture of the proposed multi-port tag is presented in Fig. 8. Note that the current located on the transmission line corresponds to traveling waves and does not radiate any power. On the other hand, the currents on the two dipoles are not traveling wave and consequently produce a radiated power. For comparison purposes, a single port tag has also been realized by using a single dipole and a single transmission line for comparison purposes. Note that both tags have been realized by hand using metallic tape placed over a PET substrate. This manual method suffers from important limitations in terms of minimum separation distance (especially with the CPS line) which affect the performance of both tags in received and backscattered power, however, both tag are affected in a similar way.

B. Multi-port Tag Characterization

Since this multi-port tag is based on a fully compliant UHF chip, tag characterization can easily be realized with commercial testbench such as Voyantic Tagformance [19] which can read the EPCID. A picture of the proposed setup is presented in Fig. 9. Note that custom testbench such as [20] could have also been used instead. In the following, the proposed multi-port tag is characterized in terms of:

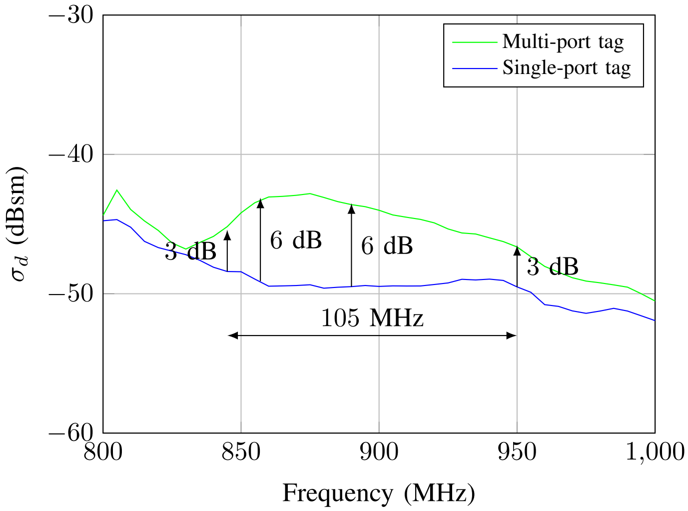

Fig. 10. Delta RCS as a function of the frequency for the proposed multi-port tag and for the single-port tag.

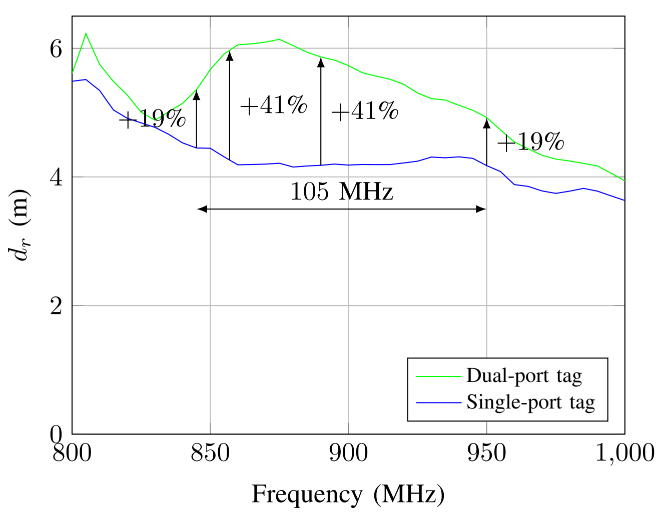

Fig. 11. Round-trip read range as a function of the frequency for the proposed multi-port tag and for the single-port tag.

- delta RCS;
- round-trip read range.

Using the commercial testbench, the backscattered power received by the reader is measured at the activation power of the tag. From this backscattered power, the delta RCS of the dual-port tag can be estimated and compared to the one of the single-port tag. Results are presented in Fig. 10 where we can see that the delta RCS of the multi-port tag outperforms the one of the single-port tag. The difference between the two tags is a function of the frequency but is higher than 6 dB between 860 and 890 MHz and higher than 3 dB between 845 and 950 MHz which is a significant result.

Moreover, the round-trip read range of the dual-port tag can be estimated from the measured delta RCS values. Results are presented in Fig. 11, assuming an equivalent radiated power of 36 dBm and a reader sensitivity of -75 dBm and an operating frequency of 915 MHz. We can see that the round-trip read range can be improved by more than 41% in the band 860–890 and by 19% in the 845 and 950 MHz band using a dual-port tag. This results is in agreement with the analytical model and the simulation results.

Finally, since the tag is based on a commercial UHF chip, it means that the tag is fully compliant with the ECP Gen2 protocol. Thus this multi-port tag can be read by any UHF reader and can participate in any inventory round with any other single-port tags.

VII. Conclusion

This paper shows that the delta RCS of a transponder can be improved if we modulate simultaneously multiple ports of its antenna. This contribution can allow tag designers to increase the delta RCS of a transponder by a factor 4 (*i.e.*, +6 dB) which corresponds to a round-trip read range improvement of 41%. The concept has been verified in simulation and measurement. The first multi-port tag fully compliant with the ECP Gen2 protocol is proposed. This multi-port tag allows one to validate the delta RCS improvement but also to be read with any UHF reader.

A natural continuation to this work will be to combine multi-port harvester and multi-port backscatter modulator into a single chip. This architecture could represent an interesting candidate for the next generation of RFID chips.

References

[1] N. Barbot, I. Prodan, and P. Nikitin, "A practical guide to optimal impedance matching for UHF RFID chip," *IEEE Journal of Radio Frequency Identification*, pp. 1–1, 2024.

[2] R. B. Green, "The general theory of antenna scattering," Ph.D. dissertation, The Ohio State University, Electrical Engineering., OH, USA, 1963.

[3] R. King and C. Harrison, "The receiving antenna," *Proceedings of the IRE*, vol. 32, no. 1, pp. 18–34, Jan. 1944.

[4] R. Hansen, "Relationships between antennas as scatterers and as radiators," *Proceedings of the IEEE*, vol. 77, no. 5, pp. 659–662, May 1989.

[5] R. Collin, "Limitations of the Thevenin and Norton equivalent circuits for a receiving antenna," *IEEE Antennas and Propagation Magazine*, vol. 45, no. 2, pp. 119–124, Apr. 2003.

[6] P. Nikitin, K. V. S. Rao, and R. D. Martinez, "Differential RCS of RFID tag," *Electron. Lett.*, vol. 43, no. 8, pp. 431–432, Apr. 2007.

[7] N. Barbot, O. Rance, and E. Perret, "Differential RCS of modulated tag," *IEEE Trans. Antennas Propag.*, vol. 69, no. 9, pp. 6128–6133, Sep. 2021.

[8] P. V. Nikitin and K. V. S. Rao, "Performance of RFID tags with multiple RF ports," in *2007 IEEE Antennas and Propagation Society International Symposium*, Honolulu, HI, Jun. 2007, pp. 5459–5462.

[9] G. Marrocco, "RFID grids: Part I – electromagnetic theory," *IEEE Transactions on Antennas and Propagation*, vol. 59, no. 3, pp. 1019–1026, Mar. 2011.

[10] S. Caizzone and G. Marrocco, "RFID grids: Part II – experimentations," *IEEE Transactions on Antennas and Propagation*, vol. 59, no. 8, pp. 2896–2904, Oct. 2011.

[11] M. B. Akbar, M. M. Morys, C. R. Valenta, and G. D. Durgin, "Range improvement of backscatter radio systems at 5.8ghz using tags with multiple antennas," in *Proceedings of the 2012 IEEE International Symposium on Antennas and Propagation*, Chicago, IL, Jul. 2012, pp. 1–2.

[12] D. M. Dobkin, T. Freed, C. Gerdom, C. Flores, E. Futak, and C. Suttner, "Cooperative tag communications," in *2015 IEEE International Conference on RFID Technology and Applications (RFID-TA)*, Tokyo, Japan, Sep. 2015, pp. 27–32.

[13] M. Mayer, B. R. Elbal, W. Gartner, R. Langwieser, and J. Kaitovic, "A flexible setup to determine RFID tag requirements for multiple-response scenarios," in *2016 IEEE International Conference on RFID (RFID)*, Orlando, FL, May 2016, pp. 1–4.

[14] G. Vougioukas, A. Bletsas, and J. N. Sahalos, "Instantaneous, zero-feedback fading mitigation with simple backscatter radio tags," *IEEE Journal of Radio Frequency Identification*, vol. 5, no. 4, pp. 451–464, Dec. 2021.
[15] N. Barbot and P. Nikitin, "Differential RCS of dual-port tag antenna with synchronous modulated backscatter," in *2024 IEEE International Conference on RFID (RFID)*, Cambridge, MA, Jun. 2024, pp. 1–6.
[16] C. A. Balanis, *Antenna theory: analysis and design*. John wiley & sons, 2016, 2nd Edition.
[17] N. Barbot and P. Nikitin, "Simple open-source UHF RFID tag platform," in *2023 IEEE International Conference on RFID (RFID)*, Seattle, WA, Jun. 2023, pp. 78–83.
[18] XArray Gateway. [Online]. Available: https://support.impinj.com/hc/en-us/articles/202755688-xArray-Gateway-Product-Brief-Datasheet
[19] Voyantic Tagformance Pro. [Online]. Available: https://voyantic.com/lab/tagformance-pro/
[20] N. Barbot and V. C. V, "Open testing and measurement bench for UHF RFID," in *2023 IEEE 13th International Conference on RFID Technology and Applications (RFID-TA)*, Aveiro, Portugal, Sep. 2023, pp. 158–161.

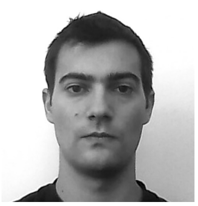

Nicolas Barbot (Member, IEEE) received the M.Sc. degree and Ph.D. degree from the University de Limoges, France in 2010 and 2013 respectively. His Ph.D. work in Xlim Laboratory was focused on error-correcting codes for the optical wireless channel. He also realized a post-doctoral work in joint source-channel decoding at L2S Laboratory, in Gif-sur-Yvette, France. Since September 2014, he has been an Assistant Professor at the Université Grenoble Alpes - Grenoble Institute of Technology, in Valence, France. His scientific background at LCIS Laboratory covers wireless communications systems based on backscattering principle which include classical RFID and chipless RFID.

His research interests include transponders which can not be described by linear time-invariant systems. This gathers harmonic transponders which are based on the use of a non-linear component (Schottky diode) or linear time-variant transponders which are based on the modification of their response in the time domain. He also places special interests on antenna design and instrumentation based on these phenomena.

Ionela Prodan (Member, IEEE) received the B.S. in Automation and Applied Informatics degree from the Univ. Politehnica of Bucharest, Romania in 2009 and her Ph.D. in Control Engineering from Supélec, Gif-sur-Yvette, France in 2012. She continued with a post-doctoral fellowship within the Chair on Systems Science and the Energetic Challenge - EDF, École Centrale Paris, France. Since 2014 she has been an Associate Professor at the Laboratory of Conception and Integration of Systems (LCIS) of Grenoble INP, Univ. Grenoble Alpes, Valence, France. She obtained her HDR (Habilitation to Conduct Research) in 2020. Her research interests are multi-disciplinary with a core expertise in control and applied mathematics. These encompass constrained optimization-based control (Model Predictive Control via distributed and decentralized approaches), mixed-integer programming, differential flatness, set-theoretic methods, and their application to motion planning for autonomous vehicles and energy management in building-scale DC microgrids. She is an Associate Editor for the EUCA European Control Conference since 2022, an Associate Editor for the IEEE Transactions on Control Systems Technology journal since 2023, and a member of the IFAC Technical Committee 6.3. Power and Energy Systems since 2020. Dr. I. Prodan is co-animator of the national French research group CT CPNL (Nonlinear Model Predictive Control) of GDR MACS, since 2021.

Pavel Nikitin (Fellow, IEEE) received the Ph.D. degree in Electrical and Computer Engineering from Carnegie Mellon University in 2002. He is currently a Principal Antenna Design Engineer with Impinj where he is doing research, design, and development of RAIN RFID tags and systems products. He previously worked at Honeywell, Intermec, IBM, and Ansys. He is also an Affiliate Associate Professor with the Electrical and Computer Engineering Department, University of Washington. He is an IEEE Fellow, received four Best Paper awards, has over 50 US patents and over 60 IEEE publications.